

OPEN ACCESS

EDITED BY

Chang Boon Peng, Nanyang Technological University, Singapore

REVIEWED BY Wenjing Wang, Qingdao University, China Faliang Luo, Ningxia University, China

*CORRESPONDENCE
Ze Xu,

□ cqteaxz@sohu.com
Yingfu Zhong,
□ cqtea1999@163.com

RECEIVED 13 May 2025 ACCEPTED 25 August 2025 PUBLISHED 08 September 2025

CITATION

Zhang Y, Wang J, Wu X, Chang R, Luo H, Yang J, Wu Q, Xu Z and Zhong Y (2025) Synthesis of carbon dots as an antibacterial and antioxidant agent. Front. Chem. 13:1627543. doi: 10.3389/fchem.2025.1627543

COPYRIGHT © 2025 Zhang, Wang, Wu, Chang, Luo, Yang,

article distributed under the terms of the Creative Commons Attribution License (CC BY). The use, distribution or reproduction in other forums is permitted, provided the original author(s) and the copyright owner(s) are credited and that the original publication in this journal is cited, in accordance with accepted academic practice. No use, distribution or reproduction is permitted which does not comply with these terms.

Wu, Xu and Zhong. This is an open-access

Synthesis of carbon dots as an antibacterial and antioxidant agent

Ying Zhang, Jie Wang, Xiuhong Wu, Rui Chang, Hongyu Luo, Juan Yang, Quan Wu, Ze Xu* and Yingfu Zhong*

Chongqing Academy of Agricultural Sciences, Chongqing, China

Objective: A new type of antibacterial and antioxidant carbon dots has been discovered.

Methods: In this study, a facile one-step hydrothermal method was employed to synthesize carbon dots (CDs) using *Yongchuan Xiuya* as the precursor.

Results: The morphology and chemical composition of the synthesized CDs were systematically characterized. The resulting doped carbon quantum dots (CDs) exhibited a spherical shape with an average particle size of 4.17 nm and a lattice spacing of 0.22 nm. The CDs demonstrated exceptional antioxidant and antibacterial properties, showing significant antimicrobial activity against both Gram-positive (*S. aureus*) and Gram-negative (*E. coli*) bacteria, with minimum inhibitory concentration values of 0.62 mg/mL and 0.85 mg/mL, respectively. Mechanistic studies revealed that bacterial cell death likely results from strong electrostatic interactions between the negatively charged bacterial surfaces and the positively charged CDs.

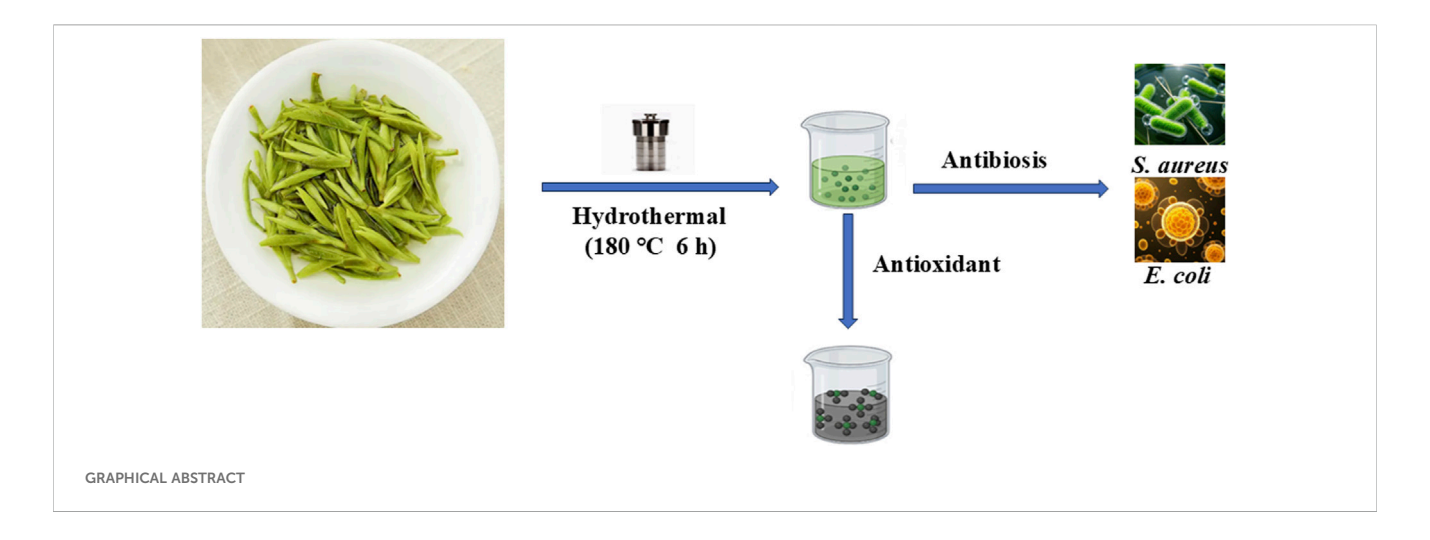
Conclusion: This work presents a cost-effective and eco-friendly approach to producing carbon dots with dual functionality as both antibacterial and antioxidant agents.

KEYWORDS

carbon dots, antibacterial, antioxidant, Yongchuan Xiuya, characterization

1 Introduction

Carbon dots (CDs), a class of zero-dimensional spherical nanoparticles with diameters typically under 10 nm (Li et al., 2023), are characterized by a core-shell structure comprising a sp²/sp³ hybridized carbon core and a surface decorated with various functional groups (Guo et al., 2022). These nanoparticles can be synthesized from diverse natural carbon precursors (Christopoulou et al., 2021) through a range of methodologies. CDs are renowned for their exceptional optical properties, including a wide emission spectrum within the visible range, high aqueous solubility, remarkable biocompatibility, and robust photostability (Chu et al., 2022; Jiang et al., 2022; Lin et al., 2022; Qu et al., 2022; Wang et al., 2022). Over the past decades, CDs have gained prominence as versatile nanomaterials for applications such as antibacterial agents and fluorescent sensors, attributed to their superior water solubility, stable fluorescence, minimal toxicity, and excellent biocompatibility (Ge et al., 2022; Wang et al., 2020; S, enol and Onganer, 2022; Fu et al., 2022; Chai et al., 2021). Recent studies have highlighted the potential of CDs as effective antibacterial agents, leveraging a synergistic interplay of multiple mechanisms to exert their antimicrobial effects (Nie et al., 2020; Pei et al., 2025; Zhao et al., 2022). Among these, the generation of reactive oxygen species (ROS)—including singlet oxygen (1O2), superoxide (O2), hydroxyl radicals (·OH), and hydrogen peroxide (H₂O₂) (Nie et al., 2020; Zhao et al., 2022; Chen et al., 2022)—plays a pivotal role in inducing oxidative stress, a primary antibacterial mechanism of CDs (Lian et al., 2024; Wang et al., 2021).



Recent studies have developed fluorescent probes with low inhibitory concentrations against *E. coli* and *S. aureus*. Among these, honeyderived carbon dots demonstrated the strongest antibacterial activity, exhibiting the lowest MIC and MBC (1.8 mg/mL) against both strains (Mohammadi et al., 2024). The methanol extract of *S. maritima* exhibited antimicrobial activity against *E. coli* (MIC = 25 mg/mL) and *S. aureus* (MIC = 6.25 mg/mL) (Can Aytar, 2024). Date syrup polyphenols exhibited antibacterial activity, with MIC values of 30 mg/mL for *E. coli* and 20 mg/mL for *S. aureus* (Taleb et al., 2016).

The escalating prevalence of bacterial infections, particularly those caused by antibiotic-resistant strains, has become a critical global health challenge, exacerbated by the misuse of antibiotics and the rapid evolution of bacterial resistance (Liu et al., 2022). This underscores the urgent need for innovative strategies to address bacterial infections. Green tea (Camellia sinensis), a member of the Theaceae family, is one of the most widely consumed beverages globally, valued for its numerous health benefits (Atak et al., 2024). *Yongchuan Xiuya*, a premium needle-shaped green tea cultivated in Yongchuan District, Chongqing, is particularly notable for its rich content of essential minerals such as potassium, calcium, magnesium, and manganese, among others (Shuai et al., 2022). This tea is celebrated for its ability to promote sodium excretion, prevent dental caries, and exert antioxidant and anti-aging effects (Tang et al., 2023).

In this study, we synthesized high-quantum-yield CDs using *Yongchuan Xiuya* as the carbon source via a hydrothermal method. The chemical composition and structural properties of the resulting CDs were thoroughly characterized. The synthesized CDs demonstrated significant antibacterial activity against both *E. coli* and *S. aureus*, highlighting their potential as novel antibacterial nanomaterials. This work provides a foundational framework for further exploration of CDs in combating bacterial infections and advancing nanomaterial-based therapeutic strategies.

2 Experimental section

2.1 Materials

All chemicals and reagents employed in this study were of analytical grade and compliant for experimental use. Yongchuan

Xiuya tea was procured from a local supermarket in Chongqing, China. Deionized water was used throughout the experiments to ensure consistency and purity. Horseradish peroxidase (HRP) was obtained from Sinopharm Chemical Reagent Co., Ltd. Phosphate buffer solution (PBS) was sourced from Merck (Darmstadt, Germany). Hydroxypropyl acrylate (HPA) and 3-(4,5-Dimethyl-2-Thiazolyl)-2,5-Diphenyl Tetrazolium Bromide (MTT) were supplied by Aladdin Co., Ltd. All materials were used as received without further purification.

2.2 Preparation of CDs

The CDs were synthesized via a one-step hydrothermal method. Briefly, 0.20 g of *Yongchuan Xiuya* tea was dispersed in 15 mL of deionized water under stirring to ensure homogeneity. The mixture was then transferred into a 25 mL Teflon-lined autoclave and subjected to hydrothermal treatment at 200 °C for 10 h. After the reaction, the autoclave was allowed to cool to room temperature naturally. The resulting suspension was centrifuged at 8,000 rpm for 10 min to remove large particles. The supernatant was further filtered through a 0.22 μm microporous membrane to obtain a clear solution. To purify the CDs, the solution was dialyzed using a dialysis bag with a molecular weight cutoff of 500 Da for 12 h to remove any unreacted precursors or small impurities. Finally, the purified CDs solution was freeze-dried to yield a solid powder, which was stored at 4 °C for subsequent characterization and applications.

2.3 Characterization

Transmission electron microscopy (TEM) images were acquired using a JEOL 2100F instrument (Tokyo, Japan) to analyze the morphology and size distribution of the synthesized CDs. Fourier-transform infrared (FT-IR) spectra were recorded on a Nicolet iS5 spectrometer (Thermo Fisher Scientific Inc., Waltham, MA, USA) to identify the functional groups present on the surface of the CDs. For detailed elemental composition analysis, X-ray photoelectron spectroscopy (XPS) was performed using an ESCALAB Xi + spectrometer (Thermo Fisher Scientific Inc.,

Waltham, MA, USA). The minimum inhibitory concentration (MIC) assay was conducted using a microplate reader from Awareness Technology (Florida, USA), with absorbance measurements taken at 600 nm. Additionally, the zeta potentials of both the CDs and bacterial cells were determined using a Nano Brook 90Plus Zeta Potential Analyzer (Malvern Instruments, UK) to assess surface charge characteristics. A relative quantum yield (QY) of CDs was determined with quinine sulfate (dispersed in 0.1 M $\rm H_2SO_4$, QY = 54%) as a reference.

2.4 Culture of bacterial

E. coli and *S. aureus* were cultured in Luria-Bertani (LB) broth medium under standard conditions. Each bacterial strain was inoculated into 5 mL of LB medium and incubated at 37 °C for 12 h with continuous shaking at 180 rpm to ensure optimal growth. The bacterial concentration was monitored by measuring the optical density at 600 nm (OD $_{600}$), and cultures were maintained within an OD600 range of 0.6–0.8 to ensure consistent growth phases. The bacterial suspensions were then diluted to a final concentration of 1.5×10^7 colony-forming units per milliliter (CFU/mL). Following activation, the bacterial suspensions were stored at 4 °C in a refrigerator for subsequent experimental use.

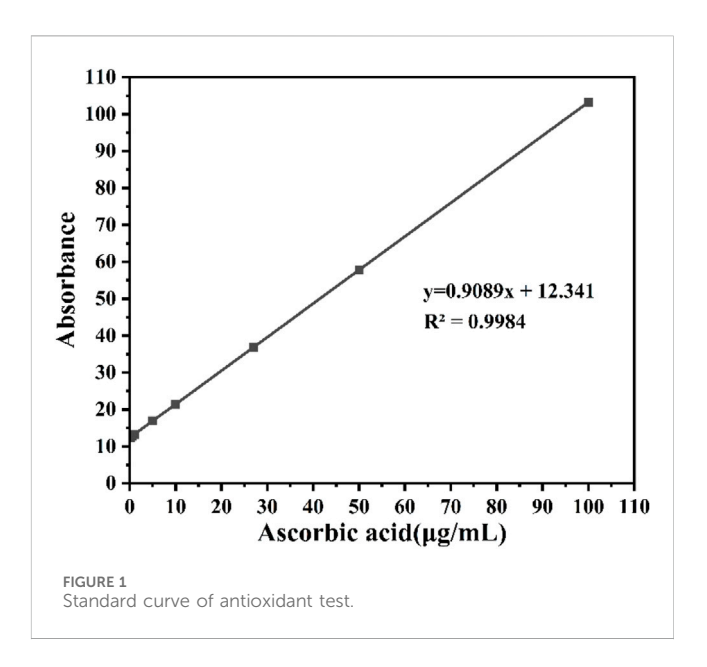
2.5 Antibacterial test

The minimum inhibitory concentration (MIC) of CDs against *E. coli* and *S. aureus* was determined using the broth microdilution method in 96-well plates. Briefly, 100 μL of bacterial suspension (1.5 \times 10 7 CFU/mL) was mixed with 100 μL of varying concentrations of CDs in the wells. The plates were then incubated at 37 °C for 12 h. After incubation, bacterial growth was quantified by measuring the optical density at 600 nm (OD600). To further assess cell viability, 10 μL of MTT (3-(4,5-dimethylthiazol-2-yl)-2,5-diphenyltetrazolium bromide) solution was added to each well, and the plates were incubated for an additional 20 min. All experiments were performed in triplicate to ensure reproducibility.

To evaluate the potential development of bacterial resistance, the initial MIC values of CDs against *E. coli* and *S. aureus* were determined. Bacteria from the 1/2 MIC concentration were then diluted to 1×10^7 CFU/mL and subjected to a 24-h incubation at 37 °C. This process was repeated daily for 14 consecutive passages, with the MIC values of the CDs-bacteria mixtures recorded at each passage. This longitudinal study aimed to monitor any changes in bacterial susceptibility to CDs over time, providing insights into the potential for resistance development.

2.6 Antibacterial mechanism of CDs

Zeta potential measurements were performed to evaluate the surface charge characteristics of the CDs and their interactions with bacterial cells. A diluted CDs solution and a mixture of the diluted CDs solution with activated bacterial suspension were analyzed using a zeta potential analyzer. This analysis provided insights



into the electrostatic interactions between the CDs and bacterial surfaces, which are critical for understanding their antibacterial mechanisms.

2.7 Antioxidant test

Antioxidant activity was evaluated by DPPH free radical scavenging capacity, and ABTS free radical scavenging capacity comparing with the equivalent antioxidant capacity (TEAC) of 6-hydroxy-2,5,7,8-tetramethylchroman-2-carboxylic acid (Trolox) and the ferric reducing antioxidant power (FRAP).

2.7.1 DPPH free radical scavenging activity

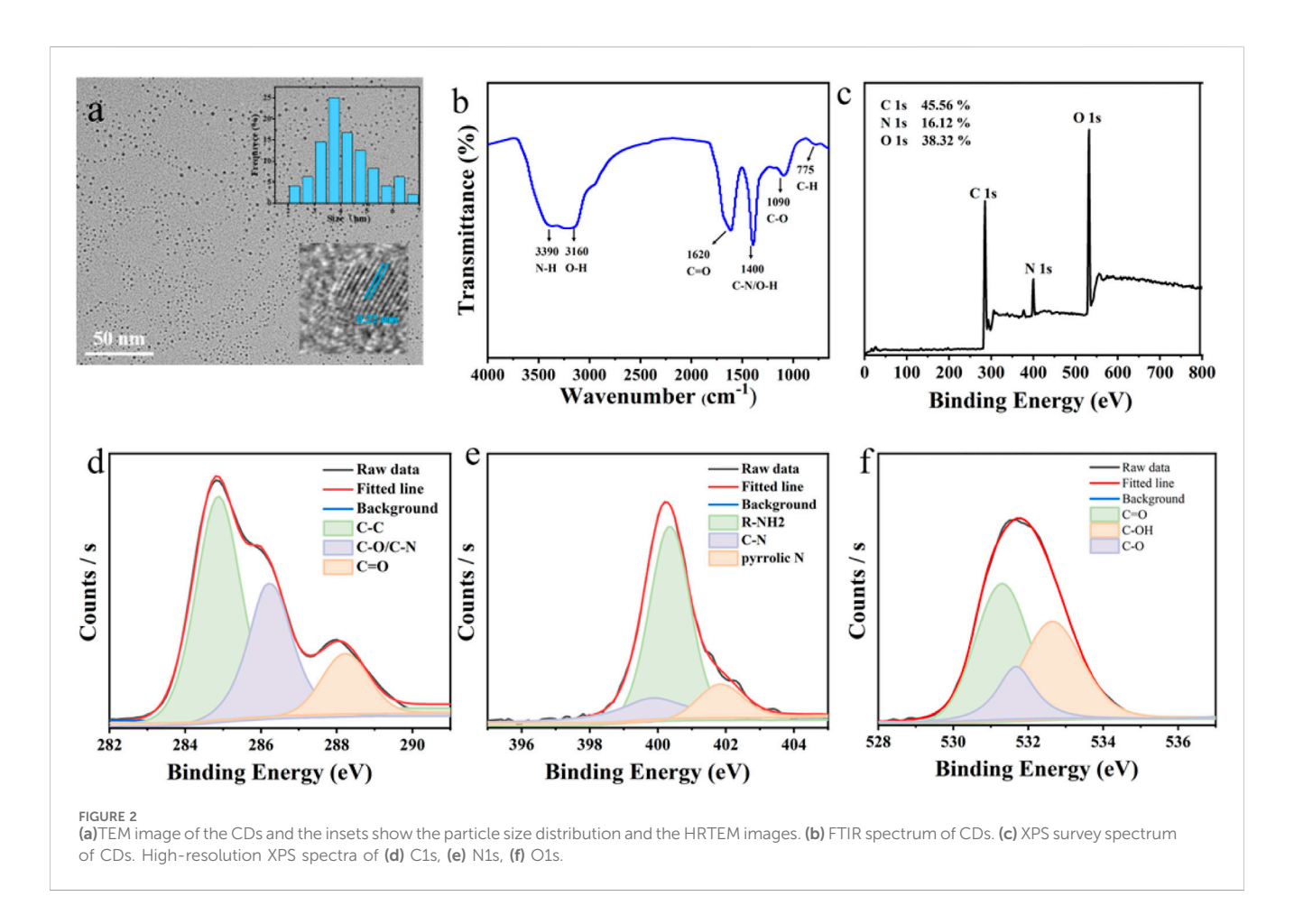
The DPPH free radical scavenging activity was measured according to Ghosh et al.'s protocol. Briefly, 200 μ L of CDs was mixed with 2,800 μ L of 0.2 mM DPPH methanolic solution. After vigorous shaking, the mixture was incubated in the dark at room temperature for 25 min. Absorbance was recorded at 517 nm using a UV–Vis spectrophotometer, with methanol as the control. Ascorbic acid was used as a standard scavenger at concentrations of 0.1, 0.5, 1, 5, 10, 27, 50, and 100 μ g/mL. A calibration curve was constructed with the equation $R^2 = 0.9984$; y = 0.9089x+12.341, where y represents the absorbance and x represents the concentration of ascorbic acid, the standard curve is shown in Figure 1. The DPPH scavenging percentage was calculated using the formula:

Free radical scavenging $\% = [(Control - Sample)/Control] \times 100$

This method provided a quantitative measure of the CDs' ability to scavenge free radicals, reflecting their antioxidant potential.

2.7.2 Ferric reducing antioxidant power (FRAP)

The antioxidant capacity assay for CDs was evaluated by the ferric reducing antioxidant power (FRAP). The FRAP reagent is a solution composed of 25 mL of 0.3 mM acetate buffer (pH 3.6), 2.5 mL of 10 mM 2,4,6-Tris (2-pyridyl)-- s-triazine (TPTZ)



dissolved in 40 mM hydrochloric acid, and 2.5 mL of 20 mM iron (III) chloride. Aliquots of FRAP solution (270 $\mu L)$ and each compound diluted in 100% methanol (30 $\mu L)$ were added to a microplate. Absorbance was read at 595 nm in a microplate reader after incubation (30 min/20 °C). Trolox (0–300 mmol) was used to create the calibration curve. The ferric reducing antioxidant potential was expressed as equivalent mmol of Trolox for each mmol of the compound tested.

2.8 Cell viability assay

Evaluation of Synthetic CDs' Protective Effects Against H_2O_2 -Induced Cell Damage. The cytoprotective effects of synthetic CDs against H_2O_2 -induced oxidative stress were analyzed using the CCK-8 assay. First, the cytotoxicity of synthetic peptides on HepG2 cells was tested. Cells were seeded in a 96-well plate (1 \times 10^4 cells/well) and cultured for 24 h at 37 °C. After replacing the medium with fresh medium containing varying peptide concentrations, the cells were incubated for an additional 12 h. The medium was then replaced with 100 μL of fresh medium containing 10 μL of CCK-8 reagent, followed by a 2 h incubation. Absorbance was measured at 450 nm. For oxidative stress protection assessment, HepG2 cells were pretreated with peptides for 12 h before exposure to 175 $\mu mol/L$ H_2O_2 for 2 h. All experiments were conducted in triplicate, and cell viability was calculated as a percentage relative to the control group.

2.9 Measurement of ROS activity

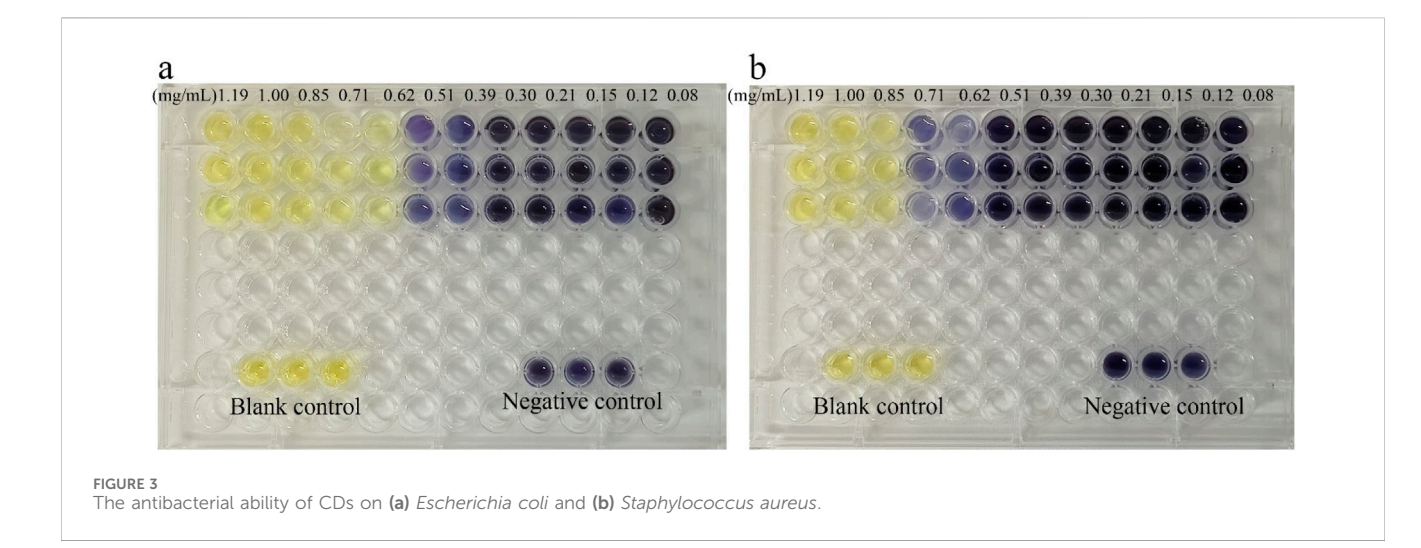
HepG2 cells from the control, model and experimental groups were collected, lysed and centrifuged at $12,000 \times g$ for 10 min at 4 °C. The supernatants were collected and analyzed using commercial assay kits following the manufacturer's instructions. ROS levels were quantified using a fluorescence-based assay.

3 Results and discussion

3.1 Characterization of CDs

The morphology and structural characteristics of the synthesized CDs were analyzed using transmission electron microscopy (TEM). As shown in Figure 2a, the CDs exhibited a particle size distribution ranging from 0.21 to 7.38 nm, with an average diameter of approximately 4.17 nm. High-resolution TEM (HRTEM) revealed a well-defined lattice spacing of 0.22 nm, indicating the crystalline nature of the CDs.

To further investigate the surface composition and functional groups of the CDs, Fourier-transform infrared (FT-IR) spectroscopy and X-ray photoelectron spectroscopy (XPS) were employed. The FT-IR spectrum (Figure 2b) displayed characteristic peaks at 3,390 cm⁻¹ and 3,160 cm⁻¹, corresponding to the stretching vibrations of N-H and O-H groups, respectively. A peak at 1,620 cm⁻¹ confirmed the presence of C=O/C=C bonds, while the peak at 1,400 cm⁻¹ was attributed to C-N/



O-H vibrations. Additionally, a peak at 775 cm⁻¹ was associated with C-H stretching.

XPS analysis (Figure 2c) revealed the elemental composition of the CDs, with C 1s (45.56%), O 1s (38.38%), and N 1s (16.12%) being the primary components. The high-resolution C 1s spectrum (Figure 2d) showed peaks at 283.8 eV and 286 eV, corresponding to C=O, C-N, and C=C bonds. The N 1s spectrum (Figure 2e) exhibited peaks at 397 eV, 399.8 eV, and 400 eV, assigned to R-NH₂, C-N-C, and N-H groups, respectively. The O 1s spectrum (Figure 2f) displayed peaks at 531.2 eV, 532.5 eV, and 534.7 eV, which were attributed to C=O, C-OH, and C-O bonds, respectively. Through elemental analysis, the elemental composition of this carbon dot was determined as follows: C: 44.73%, H: 6.12%, N: 15.35%.

Taking quinoline sulfate as a reference (Jiang et al., 2015), the quantum yield was 18.3%. These results collectively provide a comprehensive understanding of the structural and compositional properties of the synthesized CDs, highlighting their potential for various applications.

3.2 Antibacterial activity of CDs

The minimum inhibitory concentration (MIC) of the CDs was determined using a 96-well cell culture plate and the microdilution method. Bacterial suspensions of $E.\ coli$ and $S.\ aureus$ were treated with varying concentrations of CDs and incubated for 12 h under consistent conditions. Bacterial viability was assessed by measuring the optical density at 600 nm (OD₆₀₀) and comparing the values across different treatment groups.

As illustrated in Figures 3a,b, the viability of both *E. coli* and *S. aureus* decreased progressively with increasing concentrations of CDs, demonstrating a dose-dependent antibacterial effect. The MIC values, defined as the lowest concentration of CDs that completely inhibited bacterial growth, were determined to be 0.62 mg/mL for *E. coli* and 0.85 mg/mL for *S. aureus*. These results highlight the potent antibacterial activity of the CDs against both Gram-negative and Gram-positive bacteria, underscoring their potential as effective antimicrobial agents. However, the extract of *Yongchuan Xiuya* did not show excellent antibacterial effects. This indicates that after

TABLE 1 Comparison of different quantification methods to Staphylococcus aureus and Escherichia coli.

Methods	MIC _(S. aureus)	MIC _(E. coli)	References
N-CQDs/TNP	20 mg/L	20 mg/L	Zheng et al. (2024)
DS	20 mg/mL	30 mg/mL	Das et al. (2024)
Liangguoan	20 mg/mL	40 mg/mL	Zeng et al. (2021)
GEO	1 mg/mL	2 mg/mL	Wang et al. (2023)

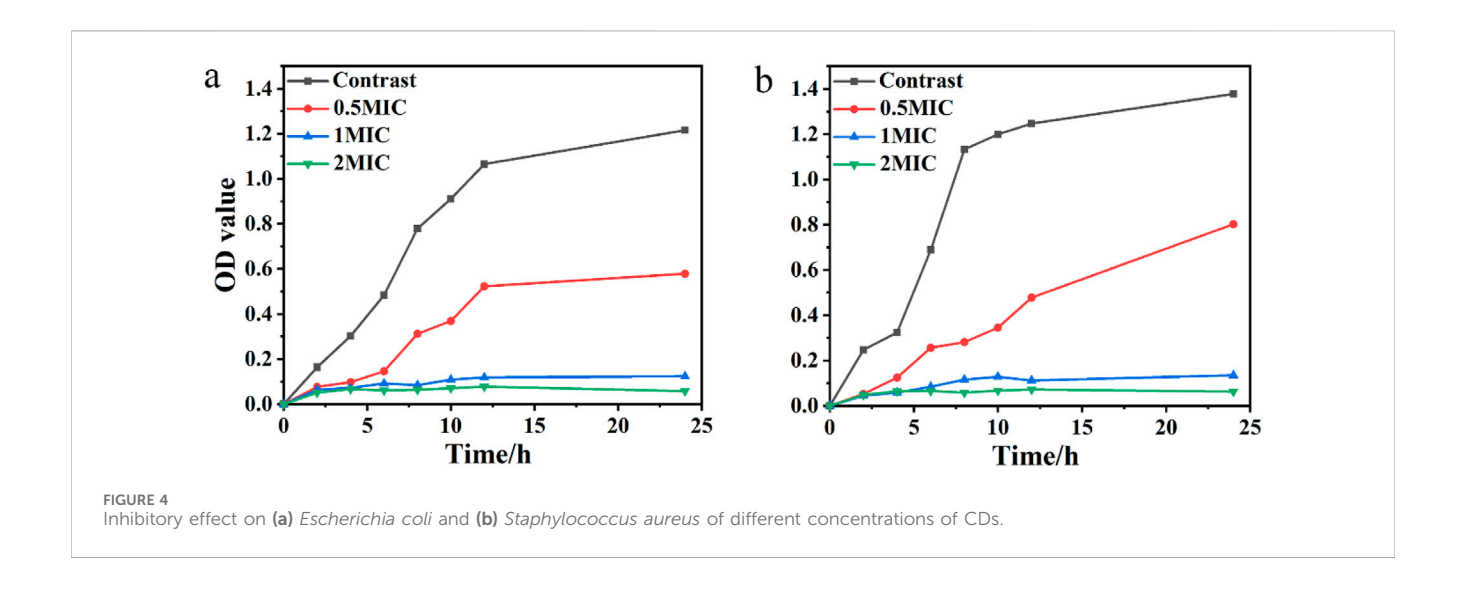
converting Yongchuan Xiuya into carbon dots, the antibacterial activity was enhanced.

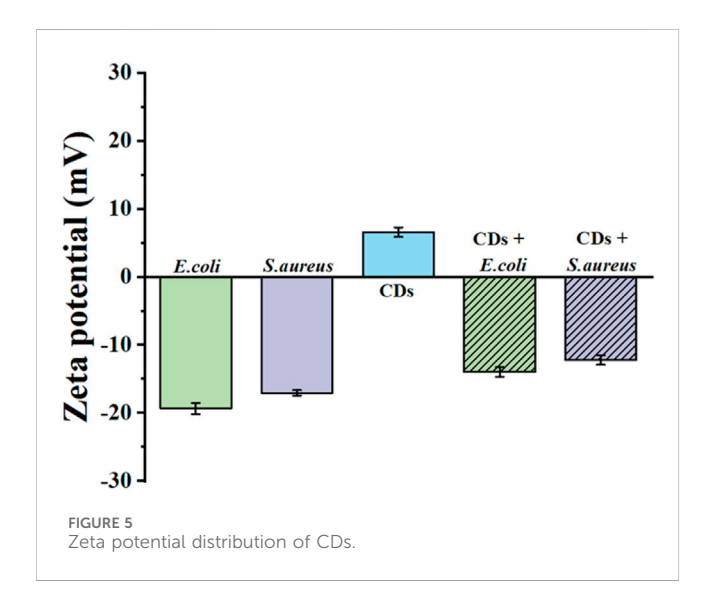
As summarized in Table 1, numerous studies have successfully synthesized fluorescent probes capable of inhibiting both Grampositive and Gram-negative pathogens at low concentrations. Notably, carbon dots exhibit significantly enhanced antibacterial activity compared to other tested compounds.

The time-dependent antibacterial activity of the CDs was evaluated by monitoring the optical density at 600 nm (OD600) over time, as shown in Figures 4a,b. The results demonstrated that the antibacterial efficacy of the CDs was strongly concentration-dependent, with higher concentrations of CDs leading to a more significant reduction in bacterial growth. Notably, when treated with CDs at a concentration equivalent to 1× the minimum inhibitory concentration (MIC), the growth of both *E. coli* and *S. aureus* was completely inhibited within 24 h. This finding underscores the potent and rapid antibacterial action of the CDs, highlighting their potential as effective agents for controlling bacterial infections.

3.3 Antibacterial mechanism of CDs

To further investigate the antibacterial mechanism of the CDs, the zeta potential of the CDs was examined. As shown in Figure 5, the zeta potentials of both the CDs and the bacterial cells were measured. The zeta potentials of E. coli and E0. aureus were determined to be E19.63 mV and E26.76 mV, respectively, reflecting the negatively charged nature of their cell walls. In





contrast, the CDs exhibited a positive zeta potential because of the presence of cationic groups such as amino groups, facilitating their electrostatic adsorption onto the negatively charged bacterial surfaces. This interaction is a critical step in the antibacterial activity of the CDs, as it enables close contact between the CDs and the bacterial cells.

3.4 Antioxidant activity of CDs

The antioxidant activity of the CDs was evaluated using three different *in vitro* methods, DPPH (2,2-diphenyl-1picrylhydrazyl) radical scavenging and ferric reducing antioxidant power (FRAP) assay.

The objective of this experiment was to evaluate the free radical scavenging activity of the CDs using the 2,2-diphenyl-1-picrylhydrazyl (DPPH) assay. The results demonstrated that the CDs possess significant antioxidant potential, with a DPPH radical scavenging activity of $91.32\% \pm 0.31\%$. This high scavenging efficiency highlights the strong ability of the CDs to neutralize

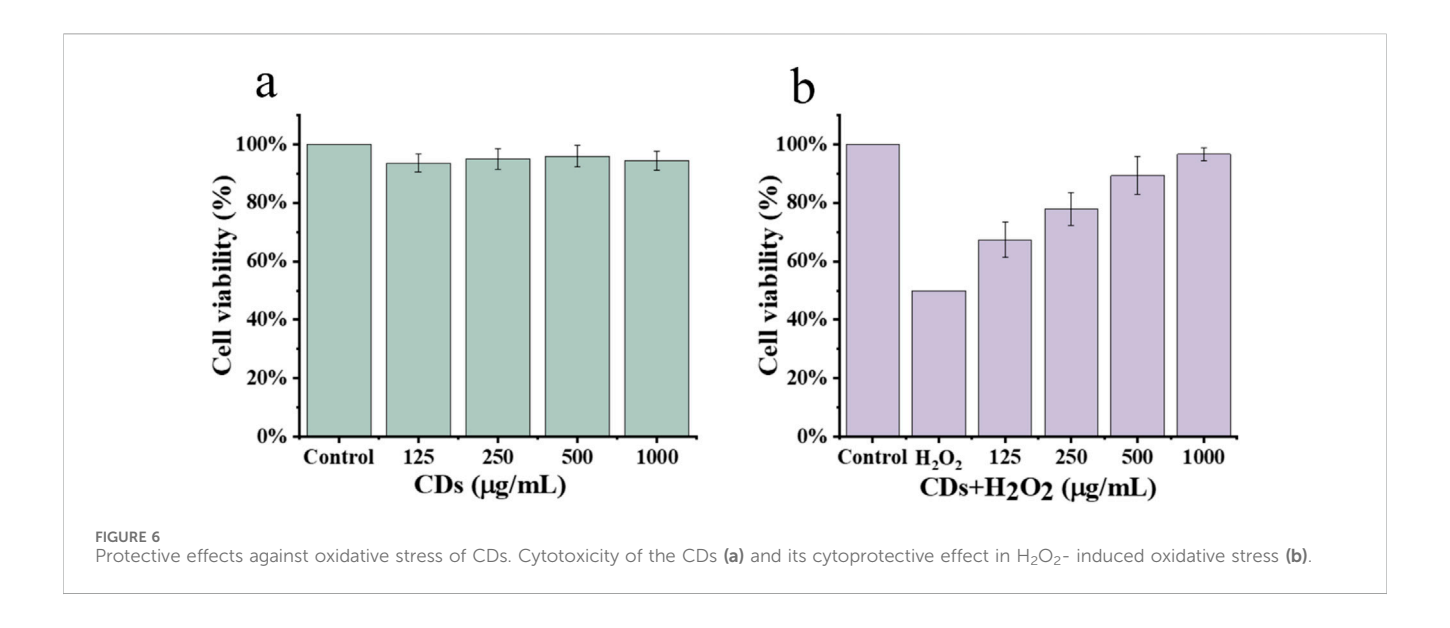
free radicals, underscoring their potential as effective antioxidant agents. These findings suggest that the CDs could be valuable in applications requiring oxidative stress mitigation, such as in biomedical or environmental contexts.

In the FRAP assay, an antioxidant reduces Fe^{3+} to Fe^{2+} by donating electrons. The reducing power of the synthesized compounds measured using the FRAP test revealed that CDs has the best-reducing capacity. The results demonstrated that the CDs possess significant antioxidant potential, with FRAP radical scavenging activity of 1,320% \pm 32%.

3.5 CDs protect HepG2 cells from H₂O₂-induced oxidative damage

HepG2 cells, derived from human hepatocellular carcinoma, are widely used for antioxidant assay of peptides in vitro. Therefore, this study employed the HepG2 cell model to evaluate the antioxidant activity of CDs. Initially, we assessed the cytotoxicity of the CDs at concentrations of 125, 250, 500, and 1,000 $\mu g/mL.$ As shown in Figure 6a, the cell viability remained above 90% at all tested concentrations, indicating that the CDs exhibited no significant cytotoxicity towards HepG2 cells at these concentrations. Therefore, the concentrations used in this study are considered safe and reasonable. Subsequently, HepG2 cells were pre-incubated with the CDs and H₂O₂ was used to simulate oxidative stress (Figure 6b). The results showed that exposure to H₂O₂ significantly decreased cell viability (p < 0.05) compared to the control group, indicating that oxidative stress induced cellular damage. In contrast, pre-incubation with CDs significantly improved cell viability in a concentration-dependent manner, demonstrating their protective effect against H2O2-induced oxidative damage.

The antioxidant effect of carbon dots can last for more than 3 days and can be explained by the hydrogen donor groups present on their surface (such as hydroxyl (-OH) and carboxyl (-COOH)). The conjugated sp² carbon structure inside the carbon dots enables the delocalization of electrons, which is conducive to the formation of free radical intermediates. The interaction between the free



radicals and the functional groups on the carbon dots leads to the formation of stable free radical adducts, effectively neutralizing reactive oxygen species (ROS). Due to the stability of the sp² carbon core and the diversity of the surface functional groups, carbon dots can maintain their antioxidant activity for a long time.

4 Conclusion

In summary, CDs were successfully synthesized via a hydrothermal method by *Yongchuan Xiuya*. Using *S. aureus* and *E. coli* as model bacteria, the CDs exhibited remarkable antioxidant and antibacterial activities. The antibacterial mechanism study revealed that bacterial cell death is likely attributed to the strong electrostatic interactions between the negatively charged bacterial surfaces and the positively charged CDs. This study presents the development of a cost-effective and environmentally friendly carbon dot material, which has been proven to possess dual functionality as both an antioxidant and an antibacterial agent.

Data availability statement

The original contributions presented in the study are included in the article/supplementary material, further inquiries can be directed to the corresponding authors.

Author contributions

YZa: Data curation, Writing – original draft. JW: Writing – original draft. XW: Investigation, Writing – original draft. RC: Validation, Writing – original draft. HL: Validation, Writing – original draft. JY: Supervision, Writing – original draft. QW: Software, Writing – original draft. ZX: Project administration, Writing – review and editing. YZo: Conceptualization, Writing – review and editing.

Funding

The author(s) declare that financial support was received for the research and/or publication of this article. This research was funded by municipal financial special project of Chongqing Academy (NO. cqaas2023sjczzd002) and Chongqing Modern Agricultural Industry Technology System (NO. CQMAITS202408).

Conflict of interest

The authors declare that the research was conducted in the absence of any commercial or financial relationships that could be construed as a potential conflict of interest.

Generative AI statement

The author(s) declare that no Generative AI was used in the creation of this manuscript.

Any alternative text (alt text) provided alongside figures in this article has been generated by Frontiers with the support of artificial intelligence and reasonable efforts have been made to ensure accuracy, including review by the authors wherever possible. If you identify any issues, please contact us.

Publisher's note

All claims expressed in this article are solely those of the authors and do not necessarily represent those of their affiliated organizations, or those of the publisher, the editors and the reviewers. Any product that may be evaluated in this article, or claim that may be made by its manufacturer, is not guaranteed or endorsed by the publisher.

References

Atak, M., Kutlu, E. Y., Çavuş, D., and Çomoğlu, M. (2024). Handmade green tea: antioxidant content and activity. *Appl. Food Res.* 4 (2), 100626. doi:10.1016/j.afres.2024. 100626

Can Aytar, E. (2024). Antioxidant and antimicrobial properties of Stachys maritima via quantum dots and molecular docking. *Chem. and Biodivers.* 21 (10), e202401057. doi:10.1002/cbdv.202401057

Chai, S., Zhou, L., Pei, S., Zhu, Z., and Chen, B. (2021). P-doped carbon quantum dots with antibacterial activity. *Micromachines* 12, 1116. doi:10.3390/mi12091116

Chen, R., Xing, Z., Lu, Y., Li, S., Song, J., Zhang, X., et al. (2022). N-doped carbon quantum dots as fluorescent probes for high-sensitivity detection of selected azo dyes. *Opt. Mater.* 131, 112630. doi:10.1016/j.optmat.2022.112630

Christopoulou, N. M., Kalogianni, D. P., and Christopoulos, T. K. C. (2021). Posidonia oceanica (mediterranean tapeweed) leaf litter as a source of fluorescent carbon dot preparations. *Microchem. J.* 161, 105787. doi:10.1016/j.microc.2020.105787

Chu, X., Chen, T., and Cao, Y. (2022). The parallel fluorescence determination of iron (III), terbium (III) and europium (III) ions using the coal-derived carbon dot. *Microchem. J.* 177, 107255. doi:10.1016/j.microc.2022.107255

Das, M. A., Patra, C., Sepay, N., Sinha, C., and Chattopadhyay, D. (2024). Comparative study on antibacterial efficacy of a series of chromone sulfonamide derivatives against drug-resistant and MDR-Isolates. *Braz. J. Microbiol.* 55 (1), 343–355. doi:10.1007/s42770-023-01194-w

Fu, L., Liu, T., Yang, F., Wu, M., Yin, C., Chen, L., et al. (2022). A multi-channel array for metal ions discrimination with animal bones derived biomass carbon dots as sensing units. *J. Photochem. Photobiol.* 424, 113638. doi:10.1016/j.jphotochem.2021.113638

Ge, G., Li, L., Chen, M., Wu, X., Yang, Y., W, D., et al. (2022). Green synthesis of nitrogen-doped carbon dots from fresh tea leaves for selective Fe3+ ions detection and cellular imaging. *Nanomaterials* 12 (6), 986. doi:10.3390/nano12060986

Guo, B., Liu, G., Hu, C., Lei, B., and Liu, Y. (2022). The structural characteristics and mechanisms of antimicrobial carbon dots: a mini review. *Mater. Adv.* 3 (21), 7726–7741. doi:10.1039/d2ma00625a

Jiang, K., Sun, S., Zhang, L., Wang, Y., Cai, C., and Lin, H. (2015). Bright-yellow-emissive N-Doped carbon dots: preparation, cellular imaging, and bifunctional sensing. ACS Appl. Mater Interfaces 7, 23231–23238. doi:10.1021/acsami.5b07255

Jiang, X., Liu, X., Wu, M., Ma, Y., Xu, X., Chen, L., et al. (2022). Facile off-on fluorescence biosensing of human papillomavirus using DNA probe coupled with sunflower seed shells carbon dots. *Microchem. J.* 181, 107742. doi:10.1016/j.microc. 2022.107742

Li, T., Dong, Y., Bateer, B., Wang, W., and Li, Z. (2023). The preparation, optical properties and applications of carbon dots derived from phenylenediamine. *Microchem. J.* 5, 108299. doi:10.1016/j.microc.2022.108299

Lian, J., Chen, B., Han, Q., Xie, H., and Xu, J. (2024). Iron ion detection and life cycle assessment of cutting fluid based on photoluminescent nitrogen-doped carbon quantum dots. *Microchem. J.* 201, 110677. doi:10.1016/j.microc.2024.110677

Lin, R., Sha, S., and Tan, M. (2022). Green synthesis of fluorescent carbon dots with antibacterial activity and their application in Atlantic mackerel (*Scomber scombrus*) storage. *Food Funct.* 13 (4), 2098–2108. doi:10.1039/d1fo03426j

Liu, Y., Xu, B., Lu, M., Li, S., Guo, J., Chen, F., et al. (2022). Ultrasmall Fe-doped carbon dots nanozymes for photoenhanced antibacterial therapy and wound healing. *Bioact. Mater.* 12, 246–256. doi:10.1016/j.bioactmat.2021.10.023

Mohammadi, S., Pashaee, A., Amini, N., Marzban, N., Harikaranahalli Puttaiah, S., Tang, V. T., et al. (2024). Green carbon dots derived from honey, garlic, and carrot: synthesis, characterization, and antibacterial properties. *Biomass Convers. Biorefinery* 15, 14823–14837. doi:10.1007/s13399-024-06349-9

Nie, X., Jiang, C., Wu, S., Chen, W., Lv, P., Wang, Q., et al. (2020). Carbon quantum dots: a bright future as photosensitizers for *in vitro* antibacterial photodynamic inactivation. *J. Photochem. Photobiol. B Biol.* 206, 111864. doi:10.1016/j.jphotobiol. 2020.111864

Pei, S., Cai, S., Yan, K., Zhou, J., Luo, K., and Chen, X. (2025). Synthesis of N-doped carbon quantum dots as an effective. Fluorescent sensor of Fe3+ ions and a potent antibacterial agent. *J. Fluoresc.* doi:10.1007/s10895-024-04112-x

Qu, Y., Li, D., Liu, J., Du, F., Tan, X., Zhou, Y., et al. (2022). Magnolia denudata leaf-derived near-infrared carbon dots as fluorescent nanoprobes for palladium(II) detection and cell imaging. *Microchem. J.* 178, 107375. doi:10.1016/j.microc.2022.107375

Shuai, M., Peng, C., Niu, H., Shao, D., Hou, R., and Cai, H. (2022). Recent techniques for the authentication of the geographical origin of tea leaves from camellia sinensis: a review. *Food Chem.* 374, 131713. doi:10.1016/j.foodchem.2021.131713

Şenol, A. M., and Onganer, Y. (2022). A novel "turn-off" fluorescent sensor based on cranberry derived carbon dots to detect iron (III) and hypochlorite ions. *J. Photochem. Photobiol.* 424, 113655. doi:10.1016/j.jphotochem.2021.113655

Taleb, H., Maddocks, S. E., Morris, R. K., and Kanekanian, A. D. (2016). The antibacterial activity of date syrup polyphenols against *S. aureus* and *E. coli. Front. Microbiol.* 7, 198. doi:10.3389/fmicb.2016.00198

Tang, Y., Wang, F., Zhao, X., Yang, G., Xu, B., Zhang, Y., et al. (2023). A nondestructive method for determination of green tea quality by hyperspectral imaging. *Food compos. Anal.* 123, 105621. doi:10.1016/j.jfca.2023.105621

Wang, H., Zhang, M., M, Y., Wang, B., Shao, M., Huang, H., et al. (2020). Selective inactivation of Gram-negative bacteria by carbon dots derived from natural biomass: Artemisia argyi leaves. *J. Mater. Chem. B* 8 (13), 2666–2672. doi:10.1039/c9tb02735a

Wang, H., Lu, F., Ma, C., Ma, Y., Zhang, M., Wang, B., et al. (2021). Carbon dots with positive surface charge from tartaric acid and m-aminophenol for selective killing of Gram-positive bacteria. *J. Mater. Chem. B* 9 (1), 125–130. doi:10.1039/d0tb02332a

Wang, J., Sun, X., Pan, W., and Wang, J. (2022). A fluorescence and phosphorescence dual-signal readout platform based on carbon dots/SiO2 for multi-channel detections of carbaryl, thiram and chlorpyrifos. *Microchem. J.* 178, 107408. doi:10.1016/j.microc. 2022.107408

Wang, H., Wang, Q., Wang, Q., Dong, W., Liu, Y., Hu, Q., et al. (2023). Metal-free nitrogen-doped carbon nanodots as an artificial nanozyme for enhanced antibacterial activity. *J. Clean. Prod.* 411, 137337. doi:10.1016/j.jclepro.2023.137337

Zeng, Y., Yu, Q., and Cheng, S. (2021). Antibacterial mechanism of liangguoan against *Staphylococcus aureus* and *Escherichia coli. Archives Microbiol.* 203 (7), 4025–4032. doi:10.1007/s00203-021-02368-6

Zhao, C., Wang, X., Yu, L., Wu, L., Hao, X., Liu, Q., et al. (2022). Quaternized carbon quantum dots with broad-spectrum antibacterial activity for the treatment of wounds infected with mixed bacteria. *Acta Biomater*. 138, 528–544. doi:10.1016/j.actbio.2021. 11.010

Zheng, Y. Y., Huang, K. T., Lee, S. J., Ni, J. S., and Hsueh, Y. H. (2024). Nitrogen-doped carbon quantum dots as antimicrobial agents against gram-positive Bacillus subtilis and *Staphylococcus aureus* under visible white light-emitting diode. *Process Biochem.* 146, 225–233. doi:10.1016/j.procbio.2024.07.024